Analytical Method for Combining the Interaction of Inlet Distortion and Turbulence

RONALD L. PANTON*
Oklahoma State University, Stillwater, Okla.

The basic assumption of the work is that the compressor rotor blades are stalling and that the flow history of the blades should be analyzed. The interaction of distortion and turbulence to produce the rotor blade flow history is shown to be essentially nonlinear. Examples are given which demonstrate that distortion factors computed on an instantaneous basis frequently do not reflect the actual blade histories. Instantaneous distortion factors can be either too high or too low depending upon the nature of the turbulence. Equations and methods are given whereby experimental data taken with a fixed rake system can be converted into a coordinate system rotating with the blades. Then it is possible to analyze the blade history for the duration and magnitude of the pressure defect. Equations are also given to compute the Fourier coefficients or the power spectral density as it would be observed by the rotor blades.

Nomenclature

a = time record length measured in rotor revolutions
A_{nm} = Fourier coefficient in rotating coordinates [Eq. (3)]
B_{nm} = Fourier coefficient in rotating coordinates [Eq. (3)]
c = airfoil chord
$C_i(\theta)$ = Fourier coefficient in fixed coordinates [Eq. (5)]
C_L = lift coefficient
$D_i(\theta)$ = Fourier coefficient in fixed coordinates [Eq. (5)]
$F_m(\hat{\theta})$ = Fourier coefficient in rotating coordinates, amplitude of fluctuation of frequency $m/2a$
i = index
I = maximum value of i
j = index
k = index indicating rake position
K = maximum value of k
n = index
N = maximum value of n
m = index
$p(\theta,t)$ = dependent variable indicative of local velocity, usually taken as the total pressure
$\hat{p}(\hat{\theta},\hat{t})$ = p function in rotating coordinates
P^- = amplitude of pressure defect
r = radial coordinate in fixed system
$\hat{r}$ = radial coordinate in rotating system
R = Fourier transform of $\hat{p}$
S_I,S_{II} = special symbols for complicated expressions, used in Appendix
t = time variable in fixed coordinate, one unit equal to time of one rotor revolution
$\hat{t}$ = time variable in rotating coordinates
T^- = time duration of pressure defect in blade history
V_∞ = velocity approaching an airfoil
α = angle of attack
β = exponent in correlation
θ = circumferential angle in fixed coordinate
θ_k = circumferential probe location
$\hat{\theta}$ = circumferential position in rotating coordinates
θ^- = circumferential extent of pressure defect
ω = circular frequency
δ_{ij} = Kronecker delta, $\delta_{ij}=1$ if $i=j$, $\delta_{ij}=0$ if $i\neq j$

I. Introduction

IT is well known that turbojet engines can suffer compressor stalls if the flow into the engine is nonuniform. Even if stall does not occur performance is degraded. In the analysis of these problems, the terms "distortion" and "turbulence" have come to mean space and time fluctuations of the flow at the compressor face.

Spatial distortion has always been of concern to the industry. The quality of the inlet flow was measured by distortion factors and the tolerance of the engine given as a critical value. Turbulence levels became more important as supersonic internal compression inlets were used. Also turbulence, more correctly transients, introduced by strong engine-inlet coupling in by-pass engines or rapid changes in inlet geometry or airplane maneouvers caused troubles in certain cases.

As turbulence entered the picture it was natural to modify the distortion factor concept to account for this new effect.[1-5] One approach is to compute the distortion factor on an instantaneous basis. Early reasoning was that if a severe distortion was held for a time equivalent to a rotor revolution that the steady-state criterion would apply. Currently instantaneous distortion factors are computed as frequently as every 10° of rotor revolution. Another approach is to measure the root-mean-square of the turbulence at a representative point and modify the stall criteria as a function of the turbulence level.

The major assumption behind this paper is that the rotor blades are stalling. In the absence of turbulence the distortion factors are an indirect indication of the angle-of-attack history of the rotor blades. When turbulence (time fluctuations) is imposed upon a distortion pattern the rotor angle-of-attack history is further modified. The interaction of turbulence and distortion to produce the rotor history is essentially nonlinear. Examples will be given which demonstrate this nonlinearity and the fact that instantaneous distortion factors do not accurately reflect the rotor flow history.

It is proposed to take a new point of view by inspecting the inlet flow as it would be seen by the rotor, that is, the flowfield history in a rotating coordinate system. Equations which allow rake data to be transformed into the rotor coordinate system are derived and discussed. This viewpoint should also be useful as input into the more sophisticated dynamic models of compressors.[6]

Compressor stalls and surges occur for many reasons. The assumption that the rotor blade history is important will not cover all possibilities. However, it is anticipated that the application of the methods proposed herein will correlate the data in a much wider class of cases than is currently possible.

II. Background

The front view of a compressor is shown in Fig. 1. Suppose that the compressor blade is moving into a region of distortion where the flow velocity is low. On the other hand, there might

Received October 26, 1971; revision received March 27, 1972.
Index categories: Airplane and Component Aerodynamics; Subsonic and Supersonic Airbreathing Propulsion; Airbreathing Engine Testing.

*Associate Professor; presently at The University of Texas at Austin, Austin, Texas.

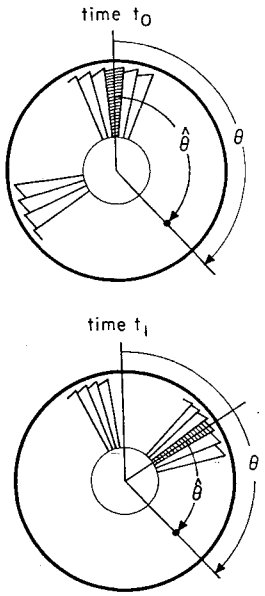

Fig. 1 Compressor face showing fixed and rotating coordinate system at two instants of time.

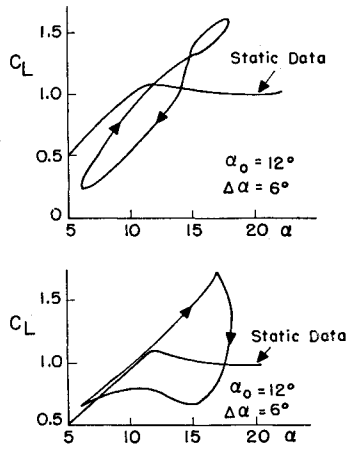

Fig. 3 Dynamic airfoil stall. Experimental data of Carta. Lower curve high frequency $\omega c/V = 0.6$. Upper curves low frequency $\omega c/V = 0.15$.

be a time fluctuation (turbulence) of the entire flow. In either case, the blade will see an unsteady flow which changes the blade angle of attack.

Figure 2 illustrates the velocity triangles for a typical blade. The flow velocity (in fixed coordinates) is completely axial as it would be ideally in a first stage without inlet guide vanes. The figure shows that a decrease in the flow velocity will increase the angle of attack. There is also a slight change in the magnitude of the relative velocity. When there are turning vanes or a preceding stator section, the flow velocity has a component in the same direction as the blade velocity. Then, a reduction in flow velocity causes a more pronounced effect on the angle and less effect on the magnitude.

Airfoils stall at a definite angle of attack under steady-state conditions. This is no longer true when a periodic oscillation in angle of attack is tested. Unsteady stall depends upon the mean angle of attack, the amplitude, and the frequency. Curves of $C_L - \alpha$ are shown for two frequencies in Fig. 3. These curves were taken from the experimental work reported by Carta.[7] High and low frequencies are characterized by the parameter $\omega c/V_\infty$. Low values of frequency parameter show the airfoil goes through periodic stalling but not along the steady-state curve. On the other hand a higher frequency might not allow time for the airfoil to stall before the angle of attack is reduced. Then a reasonably good $C_L - \alpha$ curve such as Fig. 3b is obtained. Few experimental studies of amplitude and frequency effects in stall are published.[8,9] An example of theoretical work in this area is given by Erickson[10] and by Crimi and Reeves.[11] Roberts et al.[12] recognized the frequency effect and made an interesting experimental study of compressor response to distortion. They increased the effective frequency $\omega c/V_\infty$ by increasing the chord length c. This increased the distortion tolerance of the compressor.

The importance of amplitude and frequency was recognized in defining the well-known K series of distortion factors. The key elements in these factors are the largest defect in total pressure, P^-, and the circumferential angle over which it acts, θ^-. The pressure defect indicates the velocity decrease and thus the angle of attack increase. Disturbance frequency is indirectly measured by the angular extent.

The product $P^- \cdot \theta^-$ is weighted in different ways and averaged in the radial direction. The details of the radial weighting changes from engine to engine depending upon which region is the most critical. Radial averaging gives a single number but it is not as fundamental as having a simple $P^- \cdot \theta^-$ criterion. The product essentially recognizes that frequency disturbances are more important by giving a linear weighting (θ^-) to their amplitude (P^-). Distortion factors were adequate for pure spatial distortion but have not been completely successful when there is turbulence present.[1,2,13]

To compute K-factors on an instantaneous basis or to modify the K-factor critical value according to the turbulence level does not recognize the interrelationship of turbulence and distortion. Turbulence and distortion combined in a very nonlinear way as will be shown in the next section.

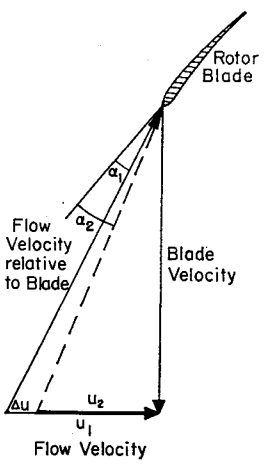

Fig. 2 Effect of decrease in flow velocity on rotor blade angle of attack.

III. Simplified Analysis

Several simple flowfields will be considered in this section. The assumed fields will be transformed into a rotor coordinate system where they will be analyzed. This will illustrate the effects on the rotor and at the same time introduce the more complete analysis of the next section.

The major indication of angle-of-attack change has generally been taken as the total pressure. This will measure the axial velocity if the static pressure is uniform and constant. The static pressure is, of course, not necessarily constant and there is currently some controversy about whether a more refined measurement is needed. This argument will be avoided by assuming the proper velocity or pressure is measured and denoted by $p(\theta,t)$. This function is the deviation from the area and time-averaged value. It is necessary to time average because the instantaneous average over the compressor face may change with time and is not necessarily the nominal design value.

The stalling rotor stage may be several stages back into the compressor. In this case $p(\theta,t)$ is still taken as an indicator of the angle-of-attack excursion at the stalling stage. This is exactly true only if the intervening stages modify the amplitude but not the frequency, i.e., the preceding stages act as a linear system.

The fixed coordinate system is r,θ,t as depicted in Fig. 1. A reference compressor blade marks the origin of the rotating system $\hat{r},\hat{\theta},\hat{t}$. A specific radial location is chosen and attention is focussed on flow pattern changes with circumferential angle and time.

For the first example consider a pure distortion where the one-per-revolution fluctuation is given by $p(\theta,t) = \cos\theta$. Transformation into the rotor coordinates is made by substituting the transformation formula

$$\theta = \hat{\theta} + 2\pi\hat{t}; \qquad t = \hat{t} \tag{1}$$

This yields

$$p(\hat{\theta},\hat{t}) = \cos\hat{\theta}\cos 2\pi\hat{t} - \sin\hat{\theta}\sin 2\pi\hat{t} \tag{2}$$

Picking a certain $\hat{\theta}$ implies observing the pressure history from a specific blade. As one expects, the circular frequency of the distortion is one cycle per revolution ($\hat{t}$ is measured in units of the time of one rotor revolution). The timing is different for each blade as given by the $\sin\hat{\theta}$ and $\cos\hat{\theta}$ terms. The blade which starts at the top has $\hat{\theta} = 0$ and the expression simplifies to $p(0,\hat{t}) = \cos 2\pi\hat{t}$. Higher mode space distortions result in higher frequencies. Since $t = \hat{t}$, pure turbulence would result in a rotor disturbance of the same frequency.

Next we consider a one-per-rev distortion plus a simple turbulence. The turbulence will have one half the amplitude of the distortion. This is not an unreasonable choice.[1,2,4] In fixed coordinates the pressure is

$$p(\theta,t) = \cos\theta + \tfrac{1}{2}\cos n\pi t$$

Pressure patterns at several times are shown in Fig. 4. Notice that the product $P^- \cdot \theta^-$ (the essential element in distortion factors) would be $1.5 \cdot \frac{4}{3}\pi = 2\pi$ for the worst instantaneous profile.

In the rotating system the pressure history for the distortion-turbulence combination is

$$\hat{p}(\hat{\theta},\hat{t}) = \cos\hat{\theta}\cos 2\pi\hat{t} - \sin\hat{\theta}\sin 2\pi\hat{t} + \tfrac{1}{2}\cos n\pi\hat{t} \tag{3}$$

Choosing the $\hat{\theta} = 0$ blade to simplify the picture

$$\hat{p}(0,\hat{t}) = \cos 2\pi\hat{t} + \tfrac{1}{2}\cos n\pi\hat{t} \tag{3a}$$

Figure 4 shows the history for several choices of "n." The blade history curves can be interpreted as an equivalent space distortion since this is a familiar concept. This is done by letting the $\hat{t} = 1$ point be $\theta = 2\pi$. For the $n = 2$ curve the product $P^- \cdot \theta^-$ is about $1.5 \cdot \frac{1}{2}(2\pi) = \frac{3}{2}\pi$. The $n = 4$ curve is much wider but not as deep, $0.75 \cdot \frac{8}{3}(2\pi) = \pi$. Both of these blade history curves would have equivalent space distortion factors less than 75% of the worst instantaneous value computed in the fixed system. In this example the actual blade history is less severe than the instantaneous distortion patterns would indicate. There are many experimental instances where the K-factors exceeded the stall criteria without stall occurring.[1,2]

Next a counter example will be presented. The rotor blade history will be more severe than the worst instantaneous distortion pattern. Consider the pattern

$$p(\theta,t) = \cos\theta + 1/2\cos 3\theta\cos 4\pi t$$

This is plotted in Fig. 5 for several values of time. For curves $t = 0$ and $\frac{1}{4}$ the product $P^- \cdot \theta^-$ is $1 \cdot \pi = \pi$ whereas for $t = \frac{1}{8}$ it is $\frac{3}{2} \cdot \frac{2}{3}\pi = \pi$.

Transforming to rotor coordinates gives the blade histories.

$$\begin{aligned}\hat{p}(\hat{\theta},\hat{t}) = {} & \cos\hat{\theta}\cos 2\pi\hat{t} - \sin\hat{\theta}\sin 2\pi\hat{t} \\ & + \tfrac{1}{4}\cos 3\hat{\theta}\,[\cos 2\pi t + \cos 10\pi t] \\ & - \tfrac{1}{4}\sin 3\hat{\theta}\,[\sin 2\pi t + \sin 10\pi t]\end{aligned} \tag{4}$$

Figure 5 shows this equation plotted for the $\hat{\theta} = 0$ blade. The equivalent distortion product is $1.5 \cdot \frac{1}{2} \cdot (2\pi) = 1.5\pi$. This is 50% more severe than the worst instantaneous pattern in fixed coordinates.

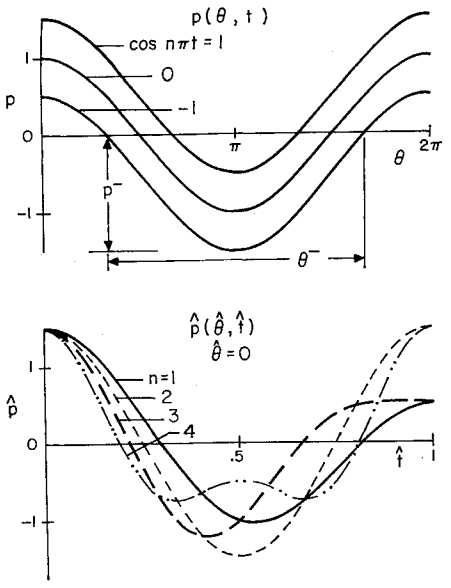

Fig. 4 Pressure patterns for distortion plus pure turbulence. Upper curves give envelope in fixed coordinates. Lower curves give histories for $\hat{\theta} = 0$ blade.

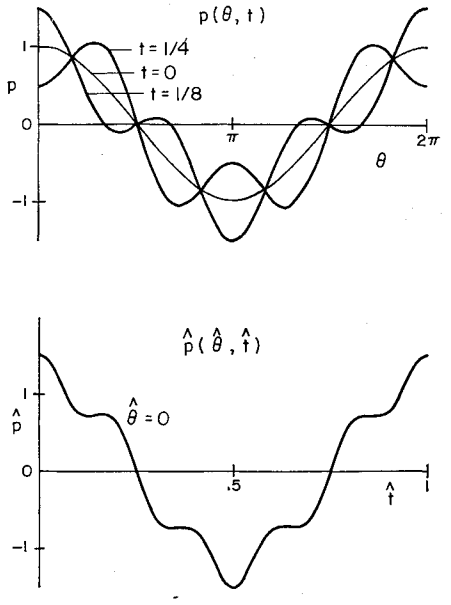

Fig. 5 Pressure patterns for distortion plus local turbulence. Upper curves give envelope in fixed coordinates. Lower curve gives history for $\hat{\theta} = 0$ blade.

From these examples it is clear that from the rotor viewpoint the effects of distortion are modified in a very nonlinear way by turbulence. Blade histories are changed with position on the rotor ($\hat{\theta}$) and may be either more or less severe than the instantaneous distortion factors would indicate.

IV. Algebraic Method for Transforming Rake Data to Rotor Coordinates

In the usual test, probes are located at several distinct circumferential locations. At each location a continuous measurement is recorded. The pressure records are

$$p(\theta_k,t) \qquad k = 0, 1, \ldots, K \tag{5}$$

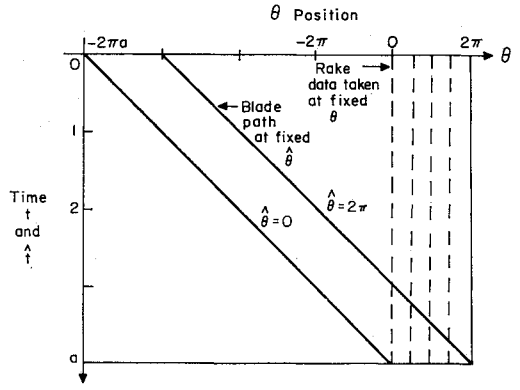

Fig. 6 Time-Theta domain for fixed and rotating coordinate systems.

where there are $K+1$ probes. Time will be measured in rotor revolutions for convenience. Figure 6 gives a sketch of the $\theta - t$ domain. Dotted lines between 0 and 2π show the location where experimental data is taken.

The time span of the records must be several rotor revolutions because low-frequency information is desired. A typical rotor revolution frequency is 160 cps. If the record length is $t_{max} = a = 4$, then 20 Hz would be the lowest frequency in the analysis. This can be verified in Eq. (7) below. The constant "a" will be restricted to be an even number for mathematical reasons (Appendix A). Once "a" is chosen, the range of θ is extended backwards to a value $\theta = -2\pi a$. In principle, the probe data from 0 to 2π is simply repeated.

The origin of the rotating coordinate system $\hat{\theta},\hat{t}$ is placed at $\theta = -2\pi a$, $t = 0$. With this choice, the region $0 \leq \hat{\theta} \leq 2\pi$ lies within the extended θ region for all times. Equations for the transformation between coordinate systems are

$$\hat{\theta} = \theta - 2\pi t + 2\pi a, \qquad \hat{t} = t \tag{6}$$

These equations will be used later.

The major goal is to analyze the fluctuating flow in the rotating coordinate system. The function $\hat{p}(\hat{\theta},\hat{t})$ can be defined to be even in $\hat{t}$ at constant $\hat{\theta}$ since negative times are of no concern. Then a Fourier series of cosines will approximate to any desired accuracy.

$$\hat{p}(\hat{\theta},\hat{t}) = \sum_{m=0}^{\infty} F_m(\hat{\theta}) \cos(m\pi\hat{t}/a) \tag{7}$$

The coefficient $F_m(\hat{\theta})$ is the amplitude of the fluctuation corresponding to the frequency $m/2a$ cycles per rotor revolution. The dependence upon the blade location $\hat{\theta}$ may wash out if a long time record is analyzed; that is, the experience of any one blade is just about like any other blade. In a stall event, however, initiation may occur over a limited number of blades. If this is true then changes with $\hat{\theta}$ would be significant. The analysis requires that the $\hat{\theta}$ dependence be accounted for explicitly. The function $F_m(\hat{\theta})$ is approximated by

$$F_m(\hat{\theta}) = \sum_{n=0}^{N} [A_{nm} \cos n\hat{\theta} + B_{nm} \sin n\hat{\theta}] \tag{8}$$

Only a finite sum is possible since experimental information is available at only a certain number of θ positions. Note that since $\sin n\hat{\theta}$ is zero for $n = 0$ that B_{om} may be taken as zero for all m.

Substitution of Eq. (3) into Eq. (2) gives

$$\hat{p}(\hat{\theta},\hat{t}) = \sum_{n=0}^{N} \sum_{m=0}^{\infty} [A_{nm} \cos n\hat{\theta} + B_{nm} \sin n\hat{\theta}] \cos(m\pi\hat{t}/a) \tag{9}$$

The task now is to convert $\hat{p}(\hat{\theta},\hat{t})$ from the rotor coordinate system to the fixed system in which the data is recorded. The coordinate transformation, Eq. (6) is substituted in Eq. (9). After considerable algebra, which is given in detail in the appendix, the following expressions result

$$p(\theta,t) = C_o(\theta) + \sum_{i=1}^{\infty} [C_i(\theta) \cos(i\pi t/a) + D_i(\theta) \sin(i\pi t/a)] \tag{10}$$

where

$$C_o(\theta) = \sum_{n=0}^{N} \tfrac{1}{2}[A_{n,2an} \cos n\theta + B_{n,2an} \sin n\theta] \tag{11}$$

$$C_i(\theta) = \sum_{n=0}^{N} \tfrac{1}{2}\{[A_{n,|i-2an|}(1 + \delta_{i,2an}) + A_{n,i+2an}] \cos n\theta + [B_{n,|i-2an|}(1 + \delta_{i,2an}) + B_{n,i+2an}] \sin n\theta\} \tag{11b}$$

$$D_i(\theta) = \sum_{n=0}^{N} \tfrac{1}{2}\{[-B_{n,|i-2an|}(1 + \delta_{i,2an}) + B_{n,i+2an}] \cos n\theta + [A_{n,|i-2an|}(1 + \delta_{i,2an}) - A_{n,i+2an}] \sin n\theta\} \tag{11c}$$

Equation (10) has purposely been constructed in the form of a Fourier series expansion of the experimental time records $p(\theta_k,t)$.

Equations (11) provide the solution to the problem of converting data taken in a stationary frame to a moving coordinate system. The analysis would proceed by first performing a Fourier analysis of each rake record. This determines the coefficients $C_i(\theta_k)$ and $D_i(\theta_k)$ at the θ_k rake position. Next the linear set of Eqs. (11) are solved to find the A_{nm}'s and B_{nm}'s. These coefficients are then summed according to Eq. (3) to give $F_m(\theta)$; the amplitude of the fluctuation at frequency $m/2a$ as observed from the rotor. The blade pressure history is given by Eq. (9).

In principle, a complete description of $p(\theta,t)$ in Eqs. (10) and (11) would require infinite sums on i and also on n. The n index has already been truncated at N since it was obvious that the rake system provides very incomplete information on θ dependence. The next task is to determine N. This must be done considering two things; we must have as many different Eqs. (11) as there are unknown A_{nm}'s and B_{nm}'s, and we must not omit any A_{nm}'s or B_{nm}'s when we plug into Eq. (8).

The manner in which the A_{nm} and B_{nm} unknowns arise in Eqs. (11) is pictured in Fig. 7. A matrix is constructed with n and m as indices. The numbers which fill the matrix are the i values in Eqs. (11) which contain A_{nm}'s and B_{nm}'s as unknowns. The figure shows a concrete example where $a = 2$ and $N = 3$. Looking at Eq. (11a) where $i = 0$ shows $A_{0,0}$, $A_{1,4}$, $A_{2,8}$, and $A_{3,12}$ (and similar B's except $B_{0,0}$) are the unknowns. Therefore, a 0 is placed in the appropriate blocks of the matrix. Proceeding to the $i = 1$ level, the unknowns are found from Eq. (11b) to be $A_{0,1}$, $A_{1,3}$, $A_{1,5}$, $A_{2,7}$, $A_{2,9}$, $A_{3,11}$ and $A_{3,13}$. Therefore 1's are placed in the proper squares. Two numbers show that certain coefficients appear in two equations as unknowns.

The more general situation is shown in Fig. 8. Lines beginning with 0, 1, ... and ending with I depict the sequence of numbers for i. When $i_{max} = I = 2aN$, the rectangle will be filled to $n = N$ and $m = 2aN$. Then the time analysis is being

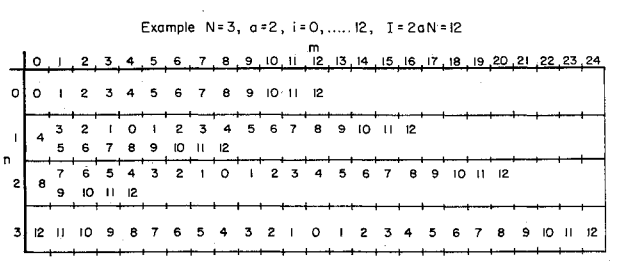

Fig. 7 Matrix of nm subscripts A_{nm} of B_{nm} in Eqs. (11). Entries are the values of i for which $m = i + 2an$ and $m = |i - 2an|$. Example for $a = 2$, $n = 3$, $i = 0, 1, \ldots, 2aN$.

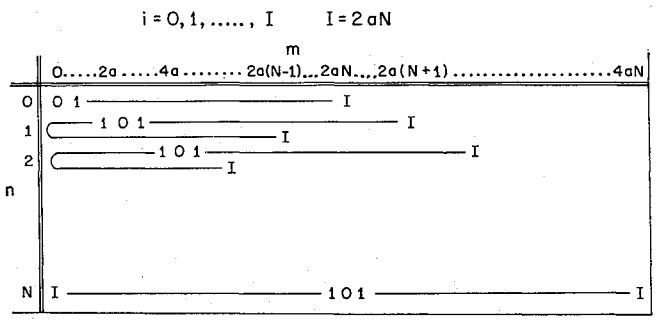

Fig. 8 Matrix of *nm* subscripts of unknown A_{nm} or B_{nm} in Eqs. (11). General case; $n = 0, 1, \ldots, N$; $i = 0, 1, \ldots, 2aN$.

carried to the same frequency as the spatial analysis. That is, the θ-variation of velocity results in a certain frequency when viewed from the rotor. Since there are a finite number of rakes, there is a finite high frequency resolution. It is possible to let I be larger than $2aN$ so that higher frequency components are extracted from the turbulence but one should realize that high frequency distortion contribution would be missing. This would not seem to be required since Plourde and Brimelow's[4] experiments show that compressor stall correlates with low frequencies.

For further discussion of the truncation problem we will take $I = 2aN$ as in Fig. 8. The number of unknown A_{nm}'s is equal to the average row length times the column length; $(3aN + 1) \cdot (N + 1)$. The number of B_{nm}'s unknowns is $(N + 1)$ less than this value since B_{0m}'s are all zero.

The number of distinct Eqs. (11) is determined by the number of rakes, $K + 1$, and highest frequency to which the data is Fourier analyzed, $I = 2aN$. When $i = 0$ there are $K + 1$ equations, and for each $i \geq 1$, $2(K + 1)$ equations. This gives a total of $(4aN + 1)(K + 1)$ equations. If this is equated to the number of unknowns, $(6aN + 1) \cdot (N + 1)$, a relation between K and N is formed. It is generally not possible, nor really desirable, to find a solution with K as integer, assuming a fixed N. At this time it appears reasonable to propose a truncation scheme where K is set equal to N. This leaves an excess of $(2aN) \cdot (N + 1)$ unknown A's and B's. The extra unknowns would be disposed of by assuming the highest frequency coefficients were zero. These frequencies are higher than the spatial resolution. Referring to Fig. 8, we set equal to zero the $aN \cdot (N + 1)$ coefficients in the triangular shaped region to the right of $m = 2aN$. This is done for both A_{nm} and B_{nm}. This reduces the system so that the equations and unknowns are equal at $(4aK + 1) \cdot (K + 1)$.

The blade pressure history $\hat{p}(\hat{\theta},\hat{t})$ or the amplitude of frequency component $m/2a$, $F_m(\hat{\theta})$, is given by Eqs. (8) and (9). Criteria for stall can be defined in terms of either of these functions. Perhaps the simplest would be to examine $\hat{p}(\hat{\theta},\hat{t})$ for the maximum negative value $\hat{P}^-$ and the duration it lasts $\hat{T}^-$. In analogy with K-factors the product $\hat{P}^- \cdot \hat{T}^-$ would be the important parameter. Since turbulence considerably widens the range of $\hat{T}^-$ of practical importance, it might be well to introduce an exponent β and examine the parameter $\hat{P}^- \cdot (\hat{T}^-)^\beta$. Stall criteria might also be established in terms of the amplitude-frequency function. The drawback of this approach is that the blade reacts to the actual pressure history which is the total of all the frequency components.

V. Fourier Transform Method

The discrete Fourier transform is widely used in analysis of digitized time signals. In recent years the numerical "Fast Fourier Transform" algorithms have reduced computational times to very reasonable values. For this reason it may be useful to recast the analysis in terms of Fourier transforms.

The mathematics will be presented in terms of continuous variables. The analogous development can be carried out in terms of discrete variables. Experimental rake data is taken at various θ locations for a certain length of time. These records are digitized and given to the computer as a matrix $p(\theta,t)$.

The rotating system is related to the fixed system by $\hat{\theta} = \theta - 2\pi t$ and $\hat{t} = t$. The pressure observed in the rotating system is formed by rearranging the matrix according to the relation

$$\hat{p}(\hat{\theta},\hat{t}) \equiv p(\hat{\theta} + 2\pi\hat{t},\hat{t}) \tag{12}$$

In order to apply the FFT one must have equal increments in $\hat{t}$. This implies a certain digitizing rate must be used such that $\theta = \hat{\theta} + 2\pi\hat{t}$ will exactly be a rake location for each $\hat{t}$. If the rakes are equally spaced this is not hard to do.

Many experiments have been conducted with very irregular rake spacings and it is not possible to obtain $p(\hat{\theta},\hat{t})$ at equal $\hat{t}$ increments. Then the data must be interpolated or a "non-fast" Fourier transform program which accepts odd increments used. Alternately, and more simple, the algebraic analysis of the previous section could be used.

The Fourier transform in the rotating system is

$$R(\hat{\theta},\hat{\omega}) = \frac{1}{(t_o)^{\frac{1}{2}}} \int_o^{t_o} \hat{p}(\hat{\theta},\hat{t}) e^{i\hat{\omega}\hat{t}} d\hat{t} \tag{13}$$

Multiplying $R(\hat{\theta},\hat{\omega})$ by its complex conjugate gives the power spectral density of fluctuations that the rotor position $\hat{\theta}$ would see. This is analogous to the amplitude-frequency relation of Eq. (9).

Stall criteria would be established by examining $\hat{p}(\hat{\theta},\hat{t})$ and/or $|R(\hat{\omega})|$. The authors inclination is to keep things as simple as possible by using the actual blade histories. The power spectrum is essentially a linear decomposition of the events. We know that dynamic airfoil stall is a very complicated and nonlinear process and should not be expected to respond to each frequency component separately.

VI. Summary and Conclusions

The angle-of-attack history of the rotor blade was assumed as the most important indicator of stall. Stalls induced by temperature effects or in stators are not included in the analysis. Equations are given which allow the blade histories and their frequency components to be calculated from distortion and turbulence data taken with conventional rake systems. These equations are very simple for equally spaced rakes, Eq. (12), and somewhat more complex for arbitrary spacing, Eqs. (8, 9, and 11).

Inspection of the equations and examples show that turbulence and distortion effects are not additive. Instantaneous distortion factors may be either too high or too low when compared to an equivalent distortion of the actual blade history.

Stall criteria based upon frequency-amplitude or power spectral density may not be as useful as a simple defect-duration correlation based upon $\hat{P}^- \cdot (\hat{T}^-)^\beta$. This argument is based upon the nonlinear behavior of dynamic airfoil stall.

Time resolution and space resolution are related. For instance, the frequency analysis of a transducer record need not be higher than the frequency than can be resolved by the rake spacing.

Testing a distortion pattern subjects the compressor to frequencies at and above the rotor frequency. Testing a pure (no distortion) turbulence pattern subjects the compressor rotor (rotor coordinates) to the same frequency as the

turbulence (fixed coordinates). Pure turbulence can be used to test the compressors sensitivity to frequencies lower than the rotor frequency. There is a slight difference in these two types of tests. In pure distortion each blade goes through the pattern at a different time, on the other hand in pure turbulence the entire cascade undergoes identical histories.

Appendix: Derivations of Eq. (6)

The derivation will be done in two parts considering the A_{nm} and B_{nm} terms separately.

Substitution of Eq. (7) into the $\cos n\theta$ terms in Eq. (9) gives

$$\sum_{n=0}^{N}\sum_{m=0}^{\infty} A_{nm}\cos[n(\theta - 2\pi t + 2\pi a)]\cos(m\pi t/a)$$

Various trigometric identities are used to expand the expression. In this step the relation $\cos(\phi + an\pi) = \cos\phi$ is employed. This is true only if we restrict a to be even

$$\sum_{n=0}^{N}\sum_{m=0}^{\infty}\frac{A_{nm}}{2}\left[\cos n\theta\cdot\cos(2an-m)\frac{\pi t}{a} + \sin\theta\cdot\sin(2an-m)\frac{\pi t}{a}\right]$$

$$+\frac{A_{nm}}{2}\left[\cos n\theta\cdot\cos(2an+m)\frac{\pi t}{a} + \sin n\theta\cdot\sin(2an+m)\frac{\pi t}{a}\right]$$

or

$$\sum_{n=0}^{N}\sum_{m=0}^{\infty}(S_{\mathrm{I}} + S_{\mathrm{II}})$$

The bracketed expressions above are defined as S_{I} and S_{II} so that they may be considered separately. Consider splitting the summation as follows

$$\sum_{n=0}^{N}\sum_{m=0}^{\infty} S_{\mathrm{I}} = \sum_{n=0}^{N}\left[\underbrace{\sum_{m=0}^{2an-1} S_{\mathrm{I}}}_{\text{a)}} + \underbrace{\tfrac{1}{2}A_{n,2an}\cos n\theta}_{\text{b)}} + \underbrace{\sum_{m=2an+1}^{\infty} S_{\mathrm{I}}}_{\text{c)}}\right]$$

Next the summation index m is replaced by i. In summation a above, let $m = 2an - i$ (if $m = 0$, $i = 2an$ and if $m = 2an - 1$, $i = 1$) and in summation c, let $m = 2an + i$. We now have

$$\sum_{n=0}^{N}\sum_{m=0}^{\infty} S_{\mathrm{I}} = \sum_{n=0}^{N}\sum_{i=1}^{2an}\tfrac{1}{2}A_{n,2an-i}\left[\cos n\theta\cdot\cos\frac{i\pi t}{a} + \sin n\theta\cdot\sin\frac{i\pi t}{a}\right] + \tfrac{1}{2}A_{n,2an}\cos n\theta +$$

$$\sum_{i=1}^{\infty}\tfrac{1}{2}A_{n,2an+i}\left[\cos n\theta\cdot\cos\frac{i\pi t}{a} - \sin n\theta\cdot\sin\frac{i\pi t}{a}\right]$$

Returning to the S_{II} sum we substitute $m = i - 2an$

$$\sum_{n=0}^{N}\sum_{m=0}^{\infty} S_{\mathrm{II}} = \sum_{n=0}^{N}\sum_{i=2an}^{\infty}\tfrac{1}{2}A_{n,i-2an}\left[\cos n\theta\cdot\cos\frac{i\pi t}{a} + \sin n\theta\cdot\sin\frac{i\pi t}{a}\right]$$

The two preceding expressions can be combined by using the absolute value sign of the indices and employing the Kronecker delta ($\delta_{ij} = 1$ if $i = j$, $\delta_{ij} = 0$ if $i \neq j$)

$$\sum_{n=0}^{N}\sum_{m=0}^{\infty}(S_{\mathrm{I}} + S_{\mathrm{II}}) = \sum_{n=0}^{N}\tfrac{1}{2}A_{n,2an}\cos n\theta +$$

$$\sum_{i=1}^{\infty}\tfrac{1}{2}[A_{n,|i-2an|}(1+\delta_{i,2an}) + A_{n,2an+i}]\cos n\theta\cdot\cos\frac{i\pi t}{a} +$$

$$\sum_{i=1}^{\infty}\tfrac{1}{2}[A_{n,|i-2an|}(1+\delta_{i,2an}) - A_{n,2an+i}]\sin n\theta\cdot\sin\frac{i\pi t}{a}$$

This result must be combined with the result of similar manipulations of the B_{nm} terms of Eq. (4). The B_{nm} terms produce the following expressions

$$\sum_{n=0}^{N}\tfrac{1}{2}B_{n,2an}\sin n\theta +$$

$$\sum_{i=1}^{\infty}\tfrac{1}{2}[B_{n,|i-2an|}(1+\delta_{n,2an}) + B_{n,2an+i}]\sin n\theta\cdot\cos\frac{i\pi t}{a} +$$

$$\sum_{i=1}^{\infty}\tfrac{1}{2}[-B_{n,|i-2an|}(1+\delta_{n,2an}) + B_{n,2an+i}]\cos n\theta\cdot\sin\frac{i\pi t}{a}$$

Collecting terms of the same frequency and rearranging will yield the equations for $C_i(\theta)$ and $D_i(\theta)$ given in Eq. (5) and Eqs. (6).

References

[1] Burcham, F. W., Jr. and Hughes, D. L., "Analysis of In-Flight Pressure Fluctuations Leading to Engine Compressor Surge in an F-111A Airplane for Mach Numbers to 2.17," AIAA Paper 70-624, San Diego, Calif., 1970.

[2] Calogeras, J. E., Burstadt, P. L., and Coltrin, R. E., "Instantaneous and Dynamic Analysis of Supersonic Inlet-Engine Compatibility," AIAA Paper 71-667, Salt Lake City, Utah, 1971.

[3] Campbell, J. L. and Ellis, S., "Inlet-Engine Compatibility Analysis," *Journal of Aircraft*, Vol. 8, No. 5, May 1971, pp. 301–307.

[4] Plourde, G. A. and Brimelow, B., "Pressure Fluctuations Cause Compressor Instability," *Proceedings of the Air Force Airframe Propulsion Compatibility Symposium*, June 1969, AFAPL-TR-69-103, June 1970.

[5] Van Deusen, E. A. and Mardoc, V. R., "Distortion and Turbulence Interaction, A Method for Evaluating Engine Inlet Compatibility," *Journal of Aircraft*, Vol. No. 1, Jan. 1972, pp. 16–22.

[6] Jansen, W., Swarden, M. C., and Carlson, A. W., "Compressor Sensitivity to Transient and Distorted Transient Flows," AIAA Paper 71-670, Salt Lake City, Utah, 1971.

[7] Carta, F. O., "Unsteady Normal Force on an Airfoil in a Periodically Stalled Inlet Flow," *Journal of Aircraft*, Vol. 4, No. 5, Sept.–Oct. 1967, pp. 416–421.

[8] Wenzel, L. M., "Experimental Investigation of the Effects of Pulse Pressure Distortions Imposed on the Inlet of a Turbofan Engine," TM-X-1928 (N70-11020), 1969, NASA.

[9] McAulay, J. E., "Effect of Dynamic Variations in Engine-Inlet Pressure on the Compression System of a Twin Spool Turbofan Engine," TM-X-2081; E-5618 (N70-39421), 1970, NASA.

[10] Erickson, L. E. and Reding, J. P., "Unsteady Airfoil Stall Review and Extension," *Journal of Aircraft*, Vol. 8, No. 8, Aug. 1971, pp. 609–616.

[11] Crimi, P. and Reeves, B. L., "A Method for Analyzing Dynamic Stall," AIAA Paper 72-37, San Diego, Calif., 1972.

[12] Roberts, F., Plourde, G. A., and Smakula, F., "Insight into Axial Compressor Response to Distortion," AIAA Paper 68-565, Cleveland, Ohio, 1968.

[13] Burcham and Bellman, "A Flight Investigation of Steady-State and Dynamic Pressure Phenomena in the Air Inlet of a Supersonic Aircraft," 38th Meeting of AGARD Propulsion and Energetics Panel, Sept. 1971, pp. 24–27.